Supporting Information

A new design of electrochromic energy storage device with high capacity, long cycle lifetime and multicolor display

Ling Wang, Mingrui Guo, Jing Zhan, Xiuling Jiao, Dairong Chen and Ting Wang**
School of Chemistry& Chemical Engineering, National Engineering Research Center for Colloidal Materials, Shandong University
E-mail:t54wang@sdu.edu.cn; cdr@sdu.edu.cn

1. Materials

Lithium perchlorate ($LiClO_4$, ACS reagent, ≥95.0 %), aluminum perchlorate ($Al(ClO_4)_3$, 98 %) and poly(3,4-ethylenedioxythiophene)-poly(styrenesulfonnate)(PEDOT:PSS) were purchased from Sigma-Aldrich. Tungsten hexachloride (WCl_6, 99.5 %), ethanol (CH_3CH_2OH), acetic acid (CH_3COOH) and isopropanol (C_3H_7OH) were purchased from Sinopharm Chemical Reagent Co. Ltd.. Titanium isopropoxide ($Ti(OC_3H_7)_4$, 99 %), vanadium triisopropoxide oxide ($VO(OC_3H_7)_3$, 96 %), propylene carbonate (PC, 99.7 %) and aluminum foil (Al, 99.9 %) were purchased from Aladdin Shanghai Aladdin Biochemical Technology Co. Ltd.. All the reagents are of analytical grade and used as-received without further purification. ITO glasses were purchased from Foshan yuanjingmei Glass Co. Ltd..

2. Film synthesis

WO_3 films: In a typical synthesis[S1], 0.5 g WCl_6 was dissolved in 5 mL anhydrous ethanol. 200 μL PEDOT: PSS was added into the solution upon sonication for 5 min. As-obtained precursor solution was then spin coated on ITO glass at 2500 rpm (Laurell model WS-650MZ-23NPP-Lite). The resultant films were subjected to UV (PSD Pro Series Digital UV Ozone System; l_{max} at 185 nm and 254 nm) irradiation for 5 min. As-obtained films were annealed in an oven (JMD-FB) in air at 110 ℃ for 1 hour.

Ti-doped V_2O_5 films: The Ti-doped V_2O_5 films were prepared by controlling the hydrolytic polycondensation of the vanadium triisopropoxide and titanium isopropoxide precursors. In a typical synthesis[S2], $VO(OC_3H_7)_3$ and $Ti(OC_3H_7)_4$ were dissolved in isopropanol separately, then 5 mL $Ti(OC_3H_7)_4$/isopropanol solution (0.14 M) was added into 10 mL $VO(OC_3H_7)_3$/isopropanol solution (0.14 M) upon continuous stirring. 300 μL acetic acid was added dropwise to tuning the hydrolytic condensation process. Within an hour, a clear and stable yellow solution can be obtained. 200 μL PEDOT: PSS were further added into the solution upon sonication. As-obtained precursor solution was then spin coated on ITO glass at 2500 rpm. As-obtained films were annealed in oven at 280 ℃ for 50 minutes.

3. Materials characterization

X-ray photoelectron spectroscopy (XPS) analyses were carried out on a Perkin-Elmer PHI-5300 ESCA system spectrometer with Al Ka radiation. The pass energy was 192 eV for the survey scan and 48 eV for the narrow scan. Powder X-ray diffraction (XRD) patterns were collected on a Rigaku D/Max 2200PC diffractometer with a graphite monochromator and Cu Kα radiation (λ= 0.15418 nm). The scanning electron microscopy (SEM, SU8010) images were collected to analyze the morphology and elemental distribution of the samples. Cross-sectional SEM images were performed on films deposited by above method about 400 nm and 600 nm of WO_3 and Ti-doped V_2O_5 films on a glass substrate.

4. Electrochemical and electrochromic measurements

All the electrochemical and electrochromic measurements of the WO_3 and Ti-doped V_2O_5 films were carried out on cary series UV-visible spectrophotometer (Cary 100, Agilent technologies) and electrochemical analyzer (CHI-660E; CH Instruments, Shanghai, China) in a three-electrode spectroelectrochemical cell, using the WO_3 film or Ti-doped V_2O_5 film as the working electrode, an Al foil working as the counter electrode and an Ag/AgCl working as the reference electrode, respectively. The galvanostatic charge/discharge (GCD) measurements were performed in a potential window to obtain the areal capacity of WO_3 and Ti-doped V_2O_5 cathode in a three-electrode cell with a piece of Al foil as the counter electrode and Ag/AgCl as the reference electrode, using the CHI-660E, in different electrolytes (1M $LiClO_4$/PC, 1M $Al(ClO_4)_3$/PC and mixed $LiClO_4$/$Al(ClO_4)_3$/PC, the proportion of Li^+ and Al^{3+} in the hybrid electrolyte was adjusted to 80:20). The cycle stability were performed at a current density of 0.5 mA/cm^2 in the potential window of -1.5~1.0 V (*vs* Ag^+/Ag) for WO_3 and -1.2~2.0 V (*vs* Ag^+/Ag) for Ti-doped V_2O_5 in 1M $LiClO_4$/$Al(ClO_4)_3$/PC electrolyte. In-situ optical transmittance as a function of the applied potential were obtained in a quartz cell recorded by the UV-visible spectrophotometer. The applied potentials were -1 V and 1 V for WO_3, -1.5 V and 2 V for Ti-doped V_2O_5, respectively. And the measurements of the transmittance at specified wavelengths (780 nm for WO_3 and 400 nm for Ti-doped V_2O_5) in real time were performed by the UV-visible spectrophotometer. The transmittance of the ITO glass in the electrolyte was used as the baseline. The cyclic voltammetry (CV) testing of deposited WO_3 and Ti-doped V_2O_5 electrode was performed in a three-electrode cell with a piece of Al foil as counter electrode and Ag/AgCl as reference electrode, using the CHI-660E, in the electrolytes of 1M $LiClO_4$/PC electrolyte. The electrochemical cyclic voltammetry cycle stability was measured at 50 mV s^{-1} in 1 M $LiClO_4$/PC electrolyte. Electrochemical impedance spectroscopy (EIS) was obtained by CHI-660E over a frequency range from 100 KHz to 0.1 Hz, with an AC amplitude of 10 mV in 1 M $LiClO_4$/PC

electrolyte.

The diffusion coefficients D (cm^2/s) of Al^{3+} and Li^+ in the WO_3 and Ti-doped V_2O_5 were calculated by Randles-Sevcik equation:

$I_p=kn^{3/2}AD^{1/2}cv^{1/2}$ (Equation S1)

where I_p (A) is the peak current, k is the Randles-Sevcik constant, k= 2.69*10^5, n is the transferred electron number involved in the redox process, A (cm^2) is the area of the electrode, C (mol/cm^3) is the concentration of Al^{3+} or Li^+ in the bulk solution, and v ($V\ s^{-1}$) is the scan rate.

Li-ion diffusion coefficients:

$$D_{(WO3)}=\left(\frac{I_p}{v^{1/2}}*\frac{1}{k*n^{3/2}*A*C}\right)^2 \qquad D_{(Ti\text{-}V5O2)}=\left(\frac{I_p}{v^{1/2}}*\frac{1}{k*n^{3/2}*A*C}\right)^2$$

$$=\left(0.29*\frac{1}{2.69*10^5*1^{3/2}*0.64*1}\right)^2 \qquad =\left(0.24*\frac{1}{2.69*10^5*1^{3/2}*1*1}\right)^2$$

$$=2.84*10^{-12} \qquad =7.96*10^{-13}$$

Al-ion diffusion coefficients:

$$D_{(WO3)}=\left(\frac{I_p}{v^{1/2}}*\frac{1}{k*n^{3/2}*A*C}\right)^2 \qquad D_{(Ti\text{-}V5O2)}=\left(\frac{I_p}{v^{1/2}}*\frac{1}{k*n^{3/2}*A*C}\right)^2$$

$$=\left(0.11*\frac{1}{2.69*10^5*3^{3/2}*0.49*1}\right)^2 \qquad =\left(0.12*\frac{1}{2.69*10^5*3^{3/2}*0.96*1}\right)^2$$

$$=2.72*10^{-14} \qquad =7.99*10^{-15}$$

5. Electrochromic energy storage device assembly

Electrochromic energy storage device was assembled using two pieces of ITO glass (5*5 cm^2) with WO_3 and Ti-V_2O_5 deposited on them, respectively. The Al metal frame was used as the anode, and propylene carbonate (PC) containing $LiClO_4$(0.8 M)/$Al(ClO_4)_3$(0.2 M) were used as the electrolyte. First, the two ITO electrodes and the Al metal frame (in the middle of the two ITO electrodes) were assembled as a cell. Epoxy glue was used to seal three sides of the cell. The electrolyte was injected into the cell by a syringe through the unsealed side of the cell. Before injection, the empty cell and the electrolyte in a vial were purged with dry N_2 for 15 min to drive away ambient air. The assembled device had an active area of 20.25 cm^2.

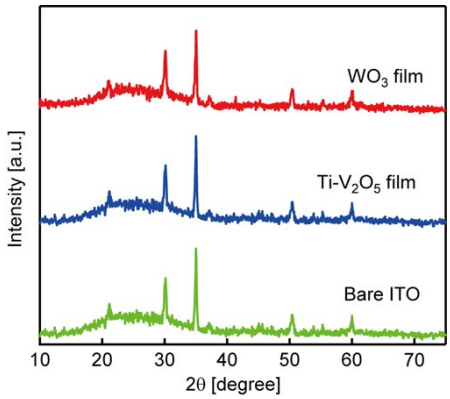

Figure S1. XRD patterns of as-prepared WO_3 and Ti-V_2O_5 films.

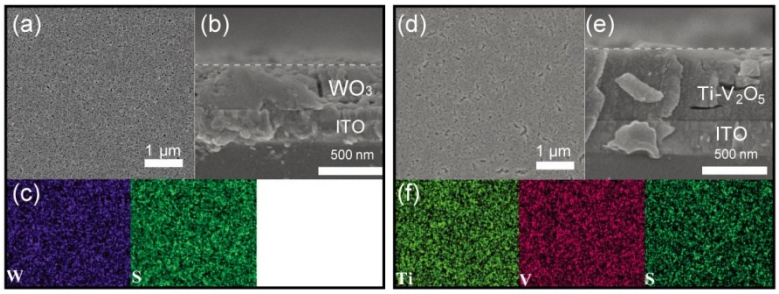

Figure S2. (a-c) SEM, cross-section SEM and the EDS elemental mappings results for the WO_3 film. (d-f) SEM, cross-section SEM and the EDS elemental mappings results for the Ti-V_2O_5 film.

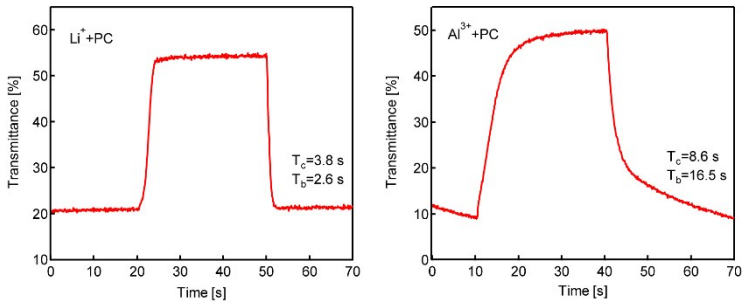

Figure S3. Real-time transmittance spectra for the Ti-V_2O_5 film in pure Li-ion and Al-ion electrolyte monitored at 400 nm.

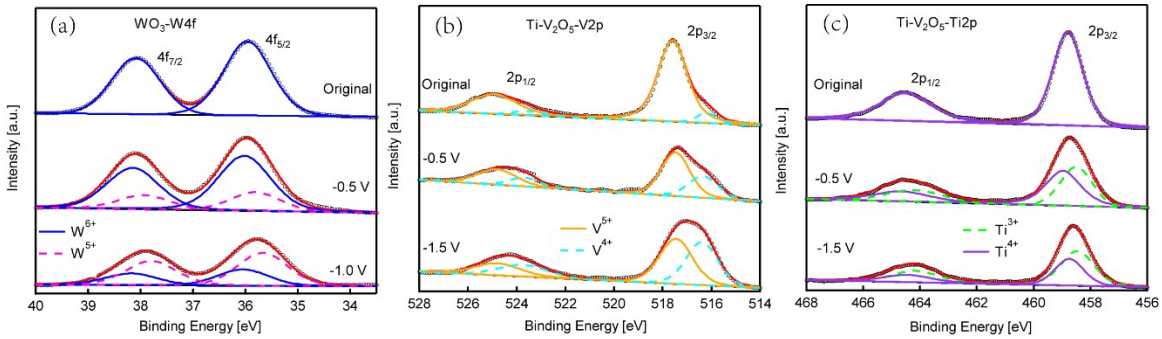

Figure S4. The ex-situ X-ray photoemission spectroscopy (XPS) spectra of the WO_3 film and the Ti-V_2O_5 film under different applied potentials. (a) The W 4f signals in the WO_3 film. (b) The V 2p signals in the Ti-V_2O_5 film. (c) The Ti 2p signals in the Ti-V_2O_5 film.

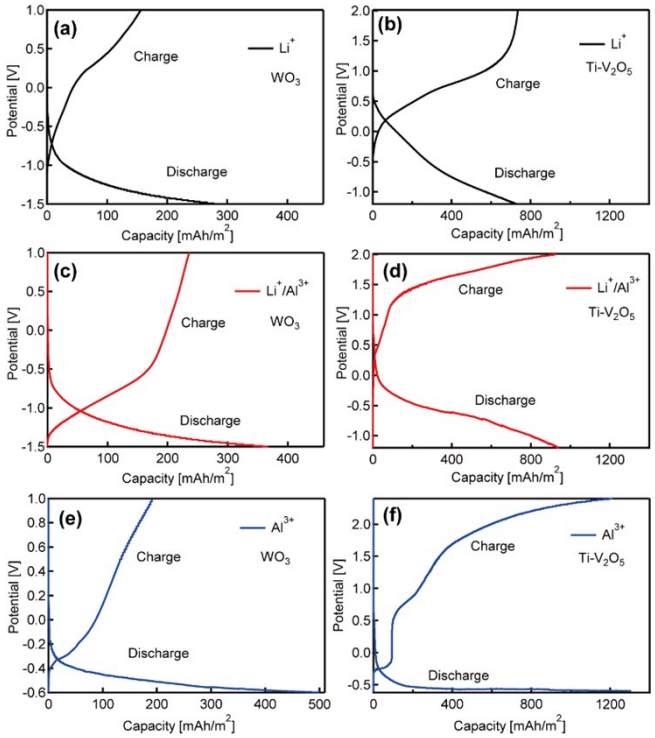

Figure S5. The first GCD profiles of the WO_3 and the Ti-V_2O_5 films in (a, b) single Li-ion electrolyte, (c, d) the mixed Li/Al-ion electrolyte and (e, f) Al-ion electrolyte at 0.5 mA/cm^2.

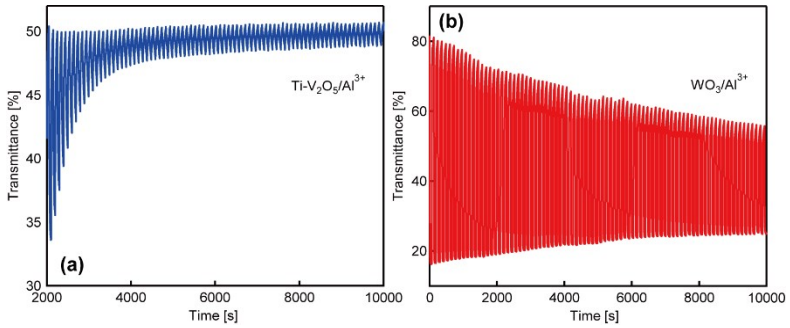

Figure S6. The cycle stability by monitoring the transmittance changes (a) at 780 nm for the WO_3 film and (b) 400 nm for the Ti-V_2O_5 film in the single Al-ion electrolyte.

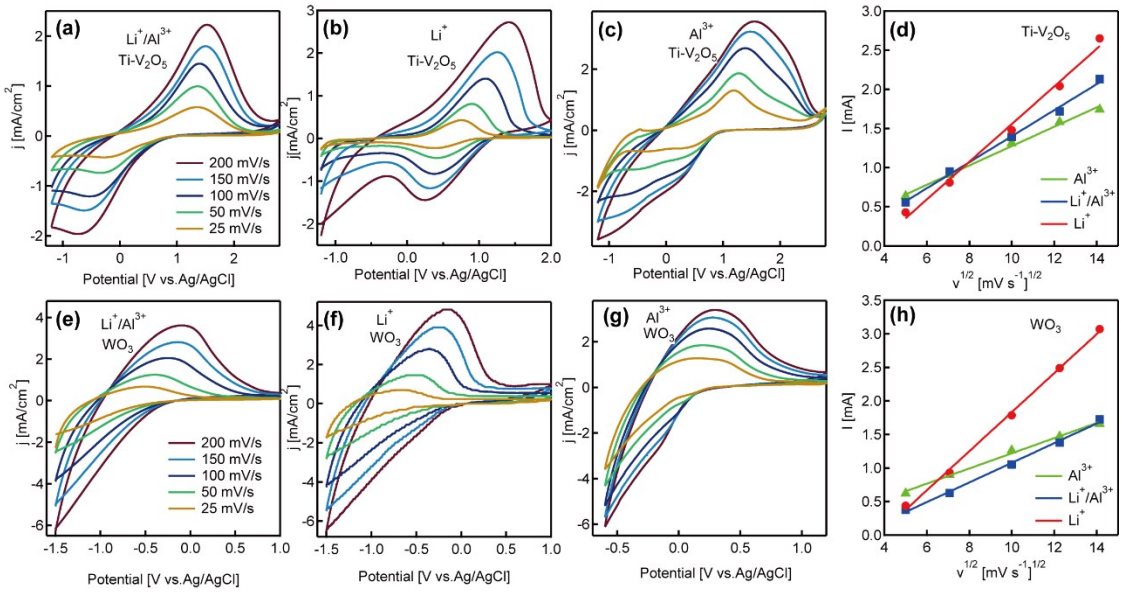

Figure S7. Cyclic voltammograms of the Ti-V_2O_5 film in (a) Li/Al-ion electrolyte, (b) Li-ion electrolyte and (c) Al-ion electrolyte at various scan rates. Cyclic voltammograms of the WO_3 film in (e) Li/Al-ion electrolyte, (f) Li-ion electrolyte and (g) Al-ion electrolyte at various scan rates. (d, h) Anodic peak current of the Ti-V_2O_5 film and the WO_3 film obtained from the cyclic voltammograms in the Li/Al-ion electrolyte, Li-ion electrolyte and Al-ion electrolyte versus the square roots of the scan rates.

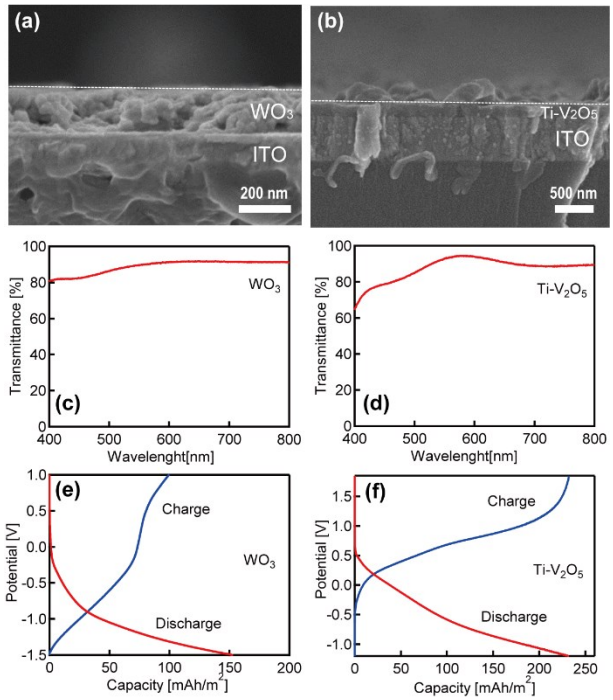

Figure S8. (a, b) Cross-section SEM images showing the thickness of the prepared thin WO_3 and Ti-V_2O_5 films. (c, d) Optical transmittance spectra of as-prepared WO_3 film and the Ti-V_2O_5 film. (e, f) The first GCD profiles of the WO_3 and the Ti-V_2O_5 films.

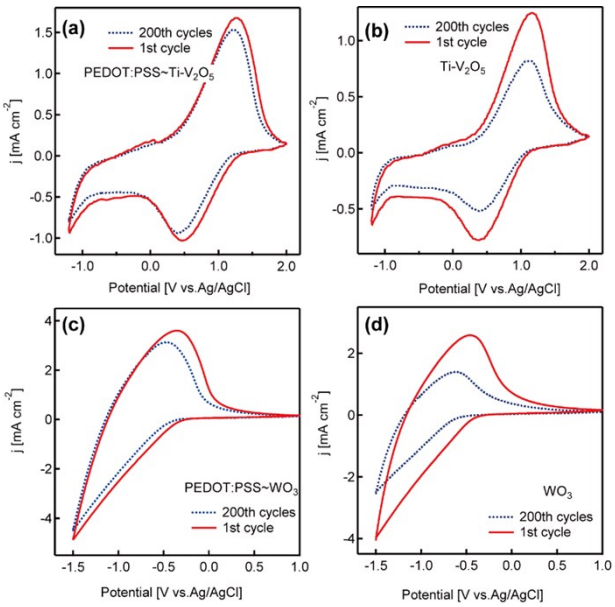

Figure S9. The electrochemical cyclic voltammetry curves of (a) Ti-V_2O_5 films with PEDOT:PSS, (b) Ti-V_2O_5 films without PEDOT:PSS,(c) WO_3 films with PEDOT:PSS,(d) WO_3 films without PEDOT:PSS, measured at 50 mV s^{-1} in 1 M $LiClO_4$/PC electrolyte.

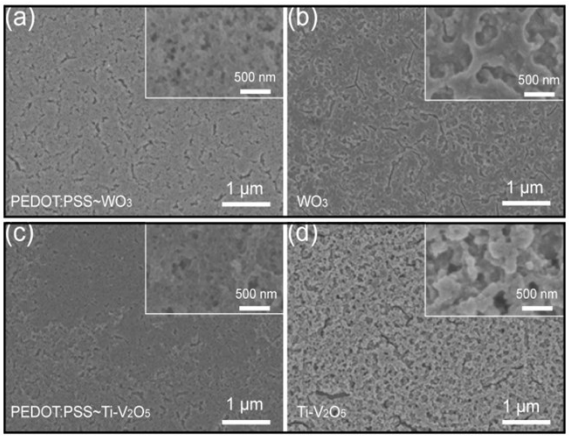

Figure S10. The SEM images of (a) WO_3 films with PEDOT:PSS, (b) WO_3 films without PEDOT: PSS, (c) Ti-V_2O_5 films with PEDOT:PSS, (d) Ti-V_2O_5 films without PEDOT:PSS, after 200 continuous cyclic voltammetry cycles.

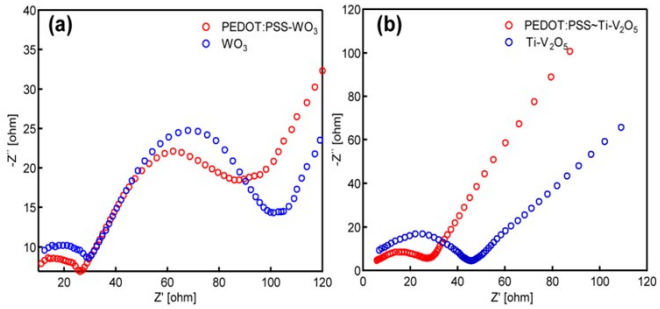

Figure S11. The electrochemical impedance spectroscopy of (a) WO_3 films with PEDOT:PSS and WO_3 films without PEDOT:PSS, (b) Ti-V_2O_5 films with PEDOT:PSS and Ti-V_2O_5 films without PEDOT:PSS, measured in 1 M $LiClO_4$/PC electrolyte.

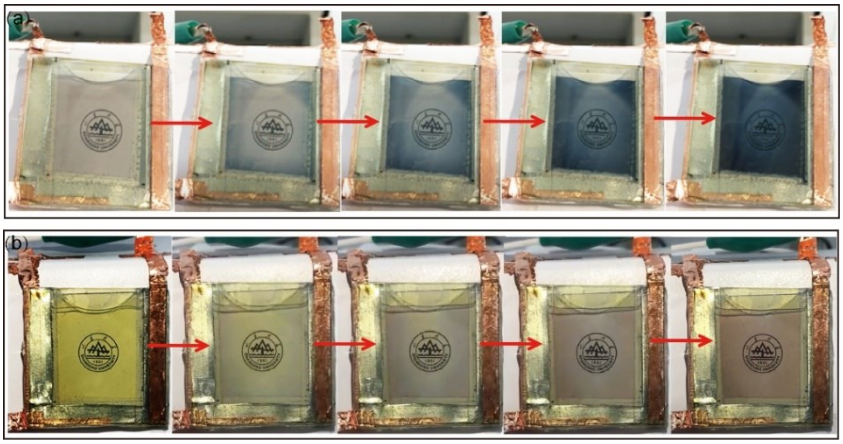

Figure S12. Color changes in photos at different times. (a) WO_3: transparent to blue, wait 20 seconds for the next photo, (b) Ti-V_2O_5: yellow to red, wait 15 seconds for the next photo.

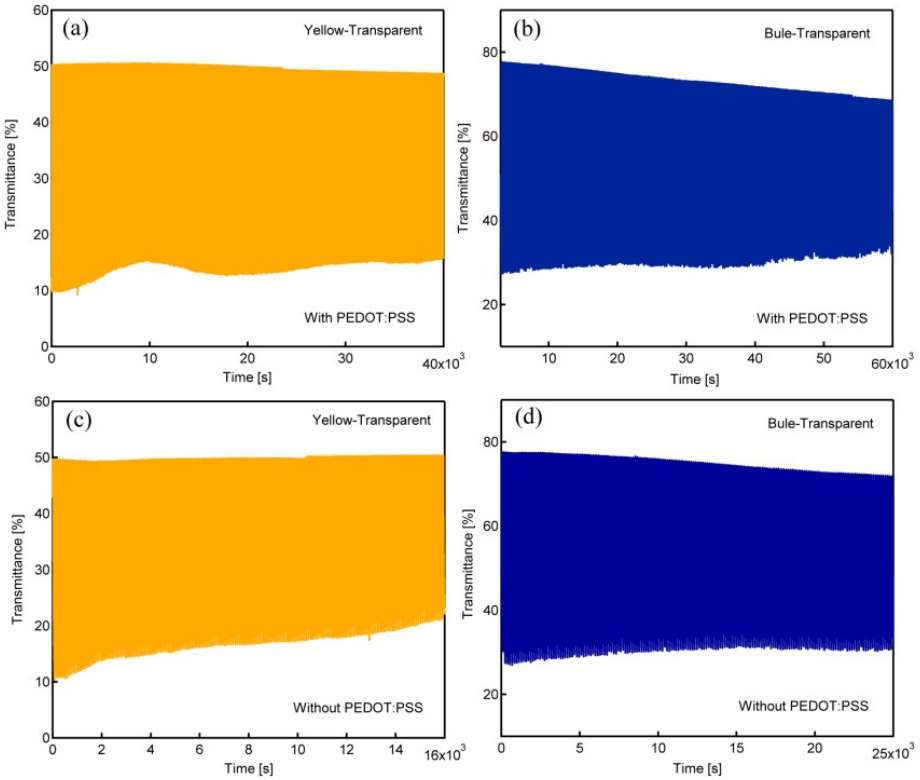

Figure S13. The cycle stability by monitoring the transmittance changes (a, c) at 400 nm and (b, d) at 780 nm for as-assembled EES device. (a, b) With PEDOT:PSS for 500 cycles. (c, d) Without PEDOT:PSS for 200 cycles.

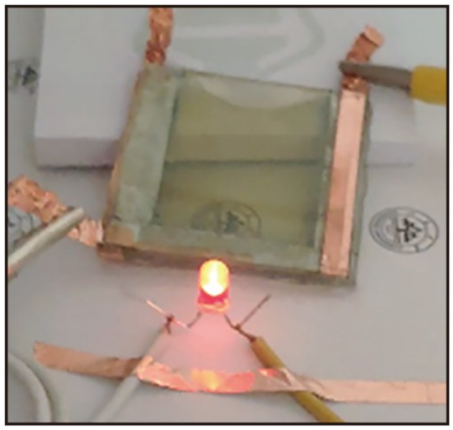

Figure S14. The yellow Ti-V_2O_5 film of the device can light an LED bulb (1.8 V, 0.04W) for 8.5 min.

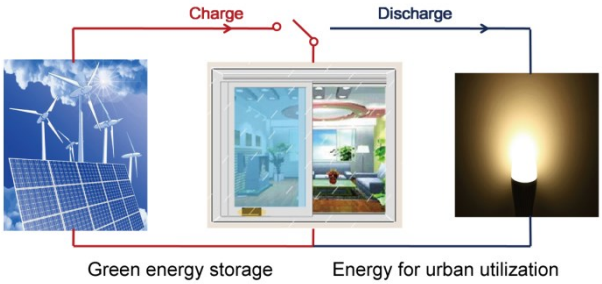

Figure S15. The EES device can be used in the storage of green energy, such as energy harvested from solar and wind, and the energy stored can be reused in urban life to reduce the energy demands

Table S1. Comparison of Current State-of-the-Art Electrochromic Films and Devices

Electrode materials	Electrolyte	Capacity	OCP(V)	Stability of charge capacity	Ref.
Al/WO_3/Ti-V_2O_5	$LiClO_4$-$Al(ClO_4)_3$/PC	933 mAh/m² in all: Al-V[a]: 631 mAh/m² Al-W[a]: 302 mAh/m²	Al-V[a]: 3.492 Al-W[a]:2.588 W-V[a]: 1.342	WO_3 film: 1000 cycles (72% capacity retention) Ti-V_2O_5 film: 1000 cycles (78% capacity retention)	This work
PLAl[b]-WO_{3-x} nanowire (~450 nm)	$LiClO_4$/PC	91 mAh/m² (0.132 Wh m^{-2})	2.59	1000 cycles (75% capacity retention)	S3
Zn-amorphous WO_3 (~300 nm)	$ZnSO_4$-$AlCl_3$aqueous	126.3 mAh/m²	1.15	2500 cycles (70% capacity retention)	S4
Zn- MTWO nanowire	$ZnSO_4$ aqueous	150 mAh/m²	1.2	100 cycles (53% capacity retention)	S5
Zn-crystalline V_3O_7 (~220 nm)	$ZnSO_4$ aqueous	15.2 mWh/g	1.38	100 cycles (40% capacity retention)	S6
Al-$W_{18}O_{49}$ nanowire	$AlCl_3$ aqueous	429 mAh/g	1.2	3 cycles (capacity loss of 18%)	S7
Al-Prussian blue (~450 nm)	KCl aqueous	75 mAh/g	1.26	50 cycles (81% capacity retention)	S8

a: Al-W: The Al anode is connected to the WO_3 ; Al-V: The Al anode is connected to the Ti-V_2O_5 ;W-V: The WO_3 is connected to the Ti-V_2O_5

b: A prelithiated Al anode.

References

S1. Moura, E. A., Cholant, C. M., Balboni, R. D. C., Westphal, T. M., Lemos, R. M. J., Azevedo, C. F., & Pawlicka, A., Electrochemical properties of thin films of V_2O_5 doped with TiO_2. *Journal of Physics and Chemistry of Solids* **2016,***119*, 1-8.

S2. Cheng, W., He, J., Dettelbach, K. E., Johnson, N. J., Sherbo, R. S., & Berlinguette, C. P., Photodeposited amorphous oxide films for electrochromic windows. *Chem* **2018,***4*(4), 821-832.

S3. Zhang, S., Cao, S., Zhang, T., Yao, Q., Lin, H., Fisher, A., & Lee, J. Y., Overcoming the technical challenges in Al anode–based electrochromic energy storage windows. *Small Methods* **2020,** *4*(1), 1900545.

S4. Li, H., Firby, C. J., & Elezzabi, A. Y., Rechargeable aqueous hybrid Zn^{2+}/Al^{3+} electrochromic batteries. *Joule* **2019,** *3*(9), 2268-2278.

S5. Li, H., McRae, L., Firby, C. J., & Elezzabi, A. Y., Rechargeable aqueous electrochromic batteries utilizing Ti-substituted tungsten molybdenum oxide based Zn^{2+} ion intercalation cathodes. *Advanced Materials* **2019,** *31*(15), 1807065.

S6. Zhang, W., Li, H., Al-Hussein, M., & Elezzabi, A. Y., Electrochromic battery displays with energy retrieval functions using solution-processable colloidal vanadium oxide nanoparticles. *Advanced Optical Materials*

2020, *8*(2), 1901224.
S7. Zhao, J., Tian, Y., Wang, Z., Cong, S., Zhou, D., Zhang, Q., & Zhao, Z., Trace H_2O_2-assisted high-capacity tungsten oxide electrochromic batteries with ultrafast charging in seconds. *Angewandte Chemie International Edition* **2016,***55*(25), 7161-7165.
S8. Wang, J., Zhang, L., Yu, L., Jiao, Z., Xie, H., Lou, X. W. D., & Sun, X. W., A bi-functional device for self-powered electrochromic window and self-rechargeable transparent battery applications. *Nature communications* **2014,***5*(1), 1-7.